Targeted inhibition of thrombin attenuates murine neonatal necrotizing enterocolitis

Kopperuncholan Namachivayam[a,b,1], Krishnan MohanKumar[a,b], Darla R. Shores[b], Sunil K. Jain[c], Jennifer Fundora[b], Allen D. Everett[b], Ling He[b], Hua Pan[d], Samuel A. Wickline[d], and Akhil Maheshwari[a,b,1]

[a]Department of Pediatrics, Morsani College of Medicine, University of South Florida, Tampa, FL 33612; [b]Department of Pediatrics, Johns Hopkins University School of Medicine, Baltimore, MD 21287; [c]Department of Pediatrics, University of Texas Medical Branch, Galveston, TX 77555; and [d]Division of Cardiology, USF Heart Institute, University of South Florida, Tampa, FL 33629

Edited by Thaddeus S. Stappenbeck, Washington University School of Medicine, St. Louis, MO, and accepted by Editorial Board Member Ruslan Medzhitov March 17, 2020 (received for review July 18, 2019)

Necrotizing enterocolitis (NEC) is an inflammatory bowel necrosis of premature infants and an orphan disease with no specific treatment. Most patients with confirmed NEC develop moderate-severe thrombocytopenia requiring one or more platelet transfusions. Here we used our neonatal murine model of NEC-related thrombocytopenia to investigate mechanisms of platelet depletion associated with this disease [K. Namachivayam, K. MohanKumar, L. Garg, B. A. Torres, A. Maheshwari, *Pediatr. Res.* 81, 817–824 (2017)]. In this model, enteral administration of immunogen trinitrobenzene sulfonate (TNBS) in 10-d-old mouse pups produces an acute necrotizing ileocolitis resembling human NEC within 24 h, and these mice developed thrombocytopenia at 12 to 15 h. We hypothesized that platelet activation and depletion occur during intestinal injury following exposure to bacterial products translocated across the damaged mucosa. Surprisingly, platelet activation began in our model 3 h after TNBS administration, antedating mucosal injury or endotoxinemia. Platelet activation was triggered by thrombin, which, in turn, was activated by tissue factor released from intestinal macrophages. Compared to adults, neonatal platelets showed enhanced sensitivity to thrombin due to higher expression of several downstream signaling mediators and the deficiency of endogenous thrombin antagonists. The expression of tissue factor in intestinal macrophages was also unique to the neonate. Targeted inhibition of thrombin by a nanomedicine-based approach was protective without increasing interstitial hemorrhages in the inflamed bowel or other organs. In support of these data, we detected increased circulating tissue factor and thrombin-antithrombin complexes in patients with NEC. Our findings show that platelet activation is an important pathophysiological event and a potential therapeutic target in NEC.

inflammation | intestinal | coagulation

Necrotizing enterocolitis (NEC) is an idiopathic, inflammatory bowel necrosis of premature infants and a leading cause of mortality in infants born between 22 and 28 wk of gestation (1–3). Premature infants who develop bacterial overgrowth and dysbiosis with a predominance of Gram-negative bacteria in their enteric microenvironment may be at enhanced risk of NEC (4–6). This risk of NEC may increase further upon exposure to environmental insults such as hypoxia and/or hypothermia, inadequate mucosal antimicrobial defenses due to immature Paneth cells, inflammation in the anemic intestine following red-blood-cell transfusions, or following enteral exposure to immunological stimulants (6–10).

Infants with a confirmed diagnosis of NEC usually develop thrombocytopenia with platelet counts $<100 \times 10^9$/L, and these low platelet counts remain an unresolved clinical dilemma. The degree and duration of thrombocytopenia in these infants correlates with the severity of bowel injury and adverse clinical outcome (11–14). The mechanism(s) of this thrombocytopenia are unclear, and these knowledge gaps are important barriers in optimizing the transfusion practices in these critically ill patients (15). To address this issue, we have developed a neonatal murine model where enteral administration of an immunological stimulant, trinitrobenzene sulfonate (TNBS), on postnatal day (P) 10 produced an acute necrotizing ileocolitis that resembled human NEC with a temporally predictable course of thrombocytopenia (1). TNBS did not induce NEC-like injury or hematological changes such as thrombocytopenia in germ-free pups (8), indicating that its inflammatory effects required intestinal microflora and were not secondary to a direct chemical/corrosive action.

TNBS has been previously used to induce colitis in adult mice (16), where it evoked enthusiasm for inducing subacute/chronic inflammation in the distal colon and for recapitulation of basal cryptitis. However, there were concerns about the artificial nature of the TNBS as a stimulus and the possibility of direct chemical effects of TNBS, a nitroaryl oxidizing acid, on the intestinal mucosa. In P10 mice, TNBS is scientifically useful as it induces an acute, temporally predictable necrotizing ileocolitis that is distinct from the more subacute colitis seen in adult rodents and strongly resembles human NEC in its ileocecal predilection, rapid progression, prominence of necrosis and macrophage-rich infiltrates, and shared signaling networks (7, 8). The rapid and highly

Significance

Necrotizing enterocolitis (NEC) is an inflammatory bowel necrosis of premature infants and is a leading cause of death in these patients. It is an orphan disease with no specific treatment. In this study, we investigated the mechanisms of NEC-related thrombocytopenia, a characteristic feature of this disease. We tested the hypothesis that platelet activation and depletion occur during NEC once mucosal disruption is well established and is secondary to bacterial translocation across the damaged mucosa. Surprisingly, platelet activation turned out to be an early thrombin-mediated pathogenetic event during NEC-like injury. We show that a targeted nanomedicine approach to inhibit thrombin can attenuate NEC-like injury. If confirmed in clinical studies, this would be a specific treatment for NEC.

Author contributions: K.N., K.M., D.R.S., S.K.J., J.F., A.D.E., H.P., S.A.W., and A.M. designed research; K.N., K.M., D.R.S., S.K.J., J.F., L.H., and H.P. performed research; K.N., K.M., S.A.W., and A.M. contributed new reagents/analytic tools; K.N., K.M., D.R.S., S.K.J., J.F., A.D.E., L.H., H.P., S.A.W., and A.M. analyzed data; and K.N., K.M., D.R.S., S.K.J., J.F., A.D.E., and A.M. wrote the paper.

The authors declare no competing interest.

This article is a PNAS Direct Submission. T.S.S. is a guest editor invited by the Editorial Board.

[1]To whom correspondence may be addressed. Email:nkcholan@jhmi.edu or akhil@jhmi.edu.

This article contains supporting information online at https://www.pnas.org/lookup/suppl/doi:10.1073/pnas.1912357117/-/DCSupplemental.

First published May 4, 2020.

predictable progression of necrotic bowel injury in the neonatal model makes it useful for the study of NEC complications such as thrombocytopenia (1). The earliest histopathological evidence of intestinal injury is detectable at 12 h and thrombocytopenia ensues at 15 to 18 h after TNBS administration (1, 7, 8, 17). Consistent with clinical observations in human NEC (18, 19), pups with TNBS-mediated acute necrotizing ileocolitis show increased immature platelet fractions, higher mean platelet volumes, and increased megakaryocyte number/ploidy in the bone marrow, findings that favor peripheral platelet consumption, not decreased production, as the kinetic basis for thrombocytopenia (1).

In the present study, we hypothesized that platelet activation, as a precursor event to platelet depletion, occurs during NEC once mucosal disruption is well established and results from the exposure to bacterial products translocated across the damaged mucosa. We posited that platelet activation and granule discharge is a secondary inflammatory event during NEC that augments mucosal damage and the associated systemic inflammatory response. Surprisingly, we found that platelet activation during NEC-like intestinal injury is an early, thrombin-mediated process that antedates both mucosal damage and the rise in bacterial products in plasma and is an important pathophysiological event during neonatal intestinal injury. Targeted inhibition of thrombin by a nanomedicine-based therapeutic approach was protective, without increasing interstitial hemorrhages in the inflamed bowel or in other organs.

Results

Platelet Activation Is an Early Event during Murine Neonatal Intestinal Injury. To investigate platelet activation in our TNBS-induced neonatal murine model of NEC (*SI Appendix*, Fig. S1*A*) (1, 7, 8, 17), we evaluated circulating platelets for three markers of activation: the activated conformation of the integrin α_{IIb}/β_3 (glycoprotein [GP] IIb/IIIa), CD31/platelet endothelial cell adhesion molecule (PECAM)-1, and P-selectin (CD62P) (Fig. 1*A*) (20). Platelet immunoreactivity for activated GPIIb/IIIa and CD31 was higher at 3 h after TNBS administration. Consistent with existing information (21), neonatal platelets expressed CD62P at low levels and upregulated it more slowly than the other two markers. At the 3-h time point, our control and NEC-like injury mice showed normal platelet counts (mean ± SE 660 ± 26 × 10^9/L vs. 664 ± 13 × 10^9/L, respectively), similar bacterial loads in ileum/proximal colon (measured by qPCR for 16S bacterial ribosomal nucleic acid [rRNA]) (*SI Appendix*, Fig. S1*B*), and had not yet developed histopathologically evident mucosal injury.

Platelets collected at the 3-h time point during NEC-like injury showed increased aggregability upon collagen exposure (Fig. 1*B*). These platelets also showed early dense granule discharge at 3 h and later, which appeared as 1) lower dense granule content upon mepacrine staining (22) (Fig. 1*C*); 2) fewer dense granules on transmission electron microscopy (Fig. 1*D*); and 3) lower ATP release following collagen stimulation in a lumi-aggregometer (*SI Appendix*, Fig. S1*C*). Unlike dense granules, the release of α-granule contents such as platelet factor (PF)-4/CXC motif ligand (CXCL) 4 seemed intermittent. Plasma CXCL4 concentrations were elevated at 6, 12, and 48 h (Fig. 1*E*). In electron micrographs, platelet α-granules were consistently depleted beyond the 18-h time point (Fig. 1*F*).

Overall, the increase in platelet activation markers, platelet hyperaggregability, and dense granule discharge within 3 h after TNBS instillation indicated that platelet activation was an early event during murine NEC-like injury. In subsequent studies, we used the activation markers (activated GPIIb/IIIa and CD31) and dense granule discharge as our two primary activation markers because these tests could be performed with smaller (20 μL) blood volumes and thereby allowed repeated measurements in pups. Platelet aggregability and ATP release provided useful information but required much larger, 250-μL blood volumes that had to be pooled from four or more pups per experiment.

Platelet Depletion Protects against Neonatal Intestinal Injury. To determine the pathogenetic importance of platelets in NEC-like intestinal injury, we subjected some pups to antibody-mediated platelet depletion before intestinal injury. Intraperitoneal administration of rat monoclonal anti-GP1bα (0.1 μg/g body weight [Fig. 2*A*]; predetermined optimum [*SI Appendix*, Fig. S2*A*]) depleted platelets overnight to 50 to 100 × 10^9/L, levels similar to those seen in moderate-severe human NEC and murine NEC-like injury (1). The intestinal bacterial loads were similar in pups with normal (*SI Appendix*, Fig. S1*B*) or depleted platelets (*SI Appendix*, Fig. S2*B*) in control and NEC-like injury groups both at enrollment and at the 3-h time point.

Platelet depletion improved survival and reduced the severity of NEC-like intestinal injury (Fig. 2 *B–D*) without increasing hemorrhages into the injured intestine (Fig. 2*E*). Mouse pups subjected to platelet depletion prior to intestinal injury showed some mucosal damage, interstitial hemorrhages, and leukocyte infiltration, but the severity of these changes was significantly lower than pups with normal platelet counts prior to intestinal injury. Consistent with the histopathological findings, mice subjected to platelet depletion prior to intestinal injury had lower plasma levels of fatty acid-binding protein (FABP)-2 (Fig. 2*F*), which is an enterocyte-derived protein biomarker of gut mucosal injury (23). These mice also showed less systemic inflammation, as evident from lower plasma C-reactive protein (CRP), CXC-motif ligand 2 (CXCL2), and serum amyloid A (SAA) (Fig. 2 *G–I*), inflammatory markers associated with human NEC and murine NEC-like injury (24).

Thrombin Activates Platelets during Neonatal Intestinal Injury. To identify the mechanism(s) underlying early platelet activation during NEC-like injury, we measured plasma thrombin activity and thrombin-antithrombin (TAT) complexes, endotoxin, thromboxane A2 (txA2), and platelet-activating factor (PAF) in a 24-h period after induction of intestinal injury. Plasma thrombin activity (Fig. 3*A*) and TAT complexes (Fig. 3*B*) were elevated at 3, 6, and 9 h after induction of intestinal injury. Endotoxin (Fig. 3*C*) and PAF levels rose later at 6 h (Fig. 3*D*), but there was no significant change in txA2 (Fig. 3*E*).

To determine the contribution of thrombin to platelet activation during NEC-like injury, we next performed a mixing experiment where we resuspended platelets from control pups in plasma from 1) control pups; 2) pups with intestinal injury at 3 h; and 3) pups with intestinal injury at 3 h with added bivalirudin, a synthetic peptide inhibitor of thrombin (25). Treatment of control platelets with plasma from intestinal injury mice increased the expression of activated GPIIb/IIIa, which was blocked by bivalirudin (Fig. 3*F*). These plasma samples also increased platelet CD31 expression and dense granule discharge (*SI Appendix*, Fig. S3 *A* and *B*). The effects of bivalirudin were recapitulated by D-phenylalanyl-prolyl-arginyl chloromethyl ketone (PPACK) (26), another synthetic inhibitor of thrombin-mediated platelet activation (*SI Appendix*, Fig. S3*C*). These findings identified thrombin as a key platelet activator during NEC-like injury.

The changes that we observed in plasma thrombin activity, TAT complexes, and other NEC-associated plasma mediators were age specific and seen only in neonates, not adults. The administration of TNBS in adult mice (n = 10 animals) did not induce any changes in NEC-related mediators at 0 to 6 h (*SI Appendix*, Fig. S3*D*).

In our neonatal model of NEC, plasma concentrations of fibrin degradation products (FDPs) rose between 12 and 24 h (*SI Appendix*, Fig. S3 *E*, *i*), indicating that platelet activation, thrombocytopenia, and thrombin generation were delayed and not likely to be a manifestation of disseminated intravascular coagulation. In regression analysis, FDP concentrations accounted for only 7.7% of the variability in platelet counts and thus did not predict thrombocytopenia in our model (*SI Appendix*, Fig. S3 *E*, *ii*).

Neonatal Platelets Are Highly Responsive to Thrombin. We next sought the mechanism(s) underlying the age-related responsiveness of neonatal platelets. Existing data suggest that neonatal platelets may show increased adhesion but may have diminished transduction of other signals (27, 28). To compare the responsiveness to thrombin, we treated mepacrine-stained platelets from P10 and adult mice with recombinant thrombin (25 μg/mL, predetermined optimum). Neonatal platelets discharged dense granules within 15 min, which was quicker than ≥30 min in adult platelets (Fig. 4*A*). Interestingly, this sensitivity of neonatal platelets was relatively specific to thrombin and was not as robust with other agents such as PAF (*SI Appendix*, Fig. S4).

To investigate the mechanism(s) for this enhanced thrombin responsiveness of neonatal platelets, we used a proteomic liquid chromatography-tandem mass spectrometry (LC-MS) platform to compare neonatal vs. adult murine platelets for key mediators of the thrombin-signaling pathway. Neonatal platelets express several thrombin-signaling proteins at higher levels than in adult platelets (29) (Fig. 4*B*), including the platelet glycoprotein-1b beta chain (GP1b beta), vasodilator-stimulated phosphoprotein (VAP), guanine nucleotide-binding protein subunit alpha 13 (G13), guanine nucleotide-binding protein (g[q] subunit alpha), cytosolic phospholipase A-2 (PLA2), phospholipase A2-activating

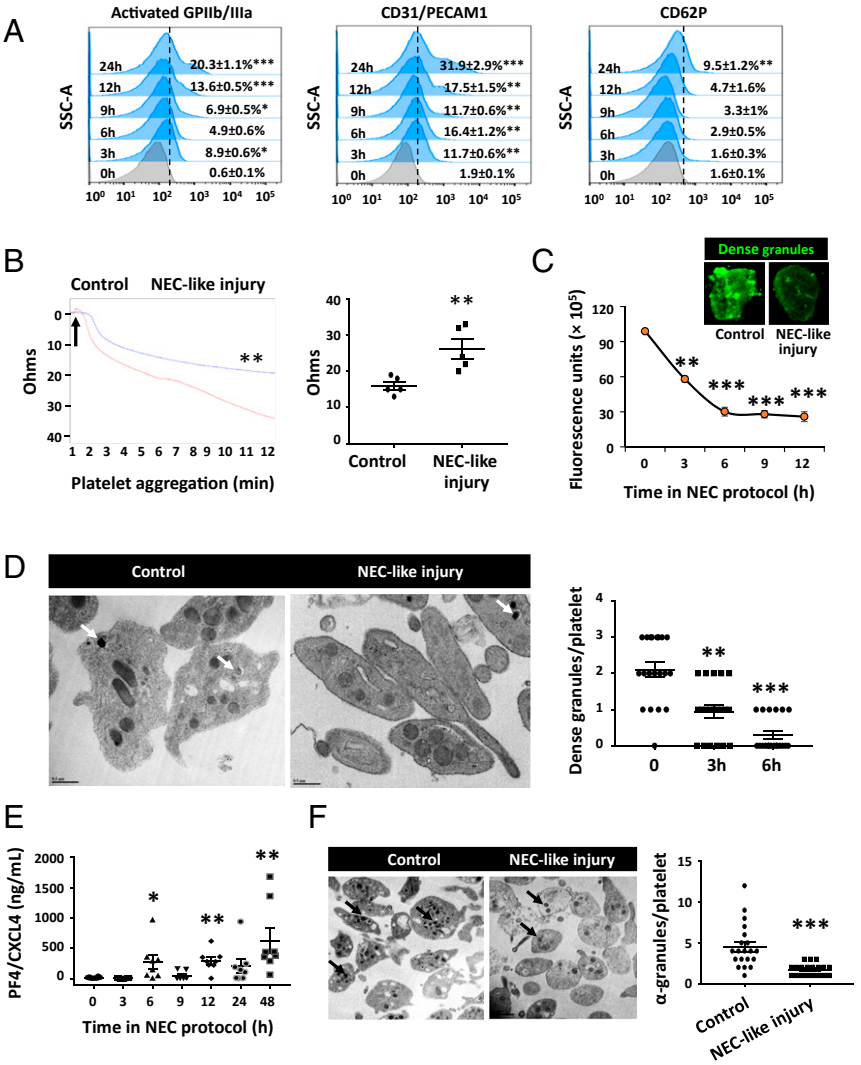

Fig. 1. Platelet activation is an early event during murine neonatal intestinal injury. (*A*) Fluorescence-activated cell-sorting histograms show platelet expression of activated GPIIb/IIIa, CD31, and P-selectin (CD62P) during intestinal injury. Controls did not change over time and have not been depicted; $n = 10$ mice/group, Kruskal–Wallis *H* test with Dunn's posttest. (*B*) Representative platelet aggregation curves (electrical impedance) measured by a lumi-aggregometer from control and intestinal injury mice (3 h after TNBS). Platelets were stimulated with collagen 2.5 μg/mL (arrow) and monitored in a lumi-aggregometer. ATP release was measured simultaneously by luminescence (*SI Appendix*, Fig. S1*B*). Scatterplots (means ± SEM) on the right summarize the slopes of the aggregation curves in the two groups; $n = 5$ samples/group; each sample was composed of blood pooled from four pups. Given statistical significance values were analyzed by Mann–Whitney *U* test. (*C*) Dense-body content of platelets during intestinal injury. Line diagram shows mepacrine fluorescence (means ± SEM) in platelets harvested at serial time points; $n = 5$ mice, 3 total blood draws/pup); Kruskal–Wallis *H* test. (*Inset*) Representative fluorescence images of mepacrine-stained platelets from control and intestinal injury (6 h) pups. (*D*) Representative transmission EM images show dense bodies (arrows) in platelets from control and intestinal injury mice 3 h after initiation of intestinal injury. Scatterplots (means ± SEM) on right summarize the dense granule count per platelet at 3 and 6 h during intestinal injury. $n = 5$ mice/group; four EM images per animal. Kruskal–Wallis *H* test. (*E*) Plasma PF4/CXCL4 concentrations (means ± SEM) measured by enzyme-linked immunosorbent assay during intestinal injury. PF4/CXCL4 concentrations were significantly higher than controls at 6, 12, and 48 h; $n = 7$ control, 11 intestinal injury mice. Kruskal–Wallis *H* test; $^*P < 0.05$; $^{**}P < 0.01$ vs. control. (*F*) Representative transmission EM images of platelets from control and intestinal injury mice at 18 h into the injury protocol show α-granules (arrows). Scatterplots on right summarize the α-granule count per platelet (means ± SEM). $n = 5$ mice/group; four EM images per animal. Mann–Whitney *U* test. $^*P < 0.05$; $^{**}P < 0.01$; $^{***}P < 0.001$ vs. control.

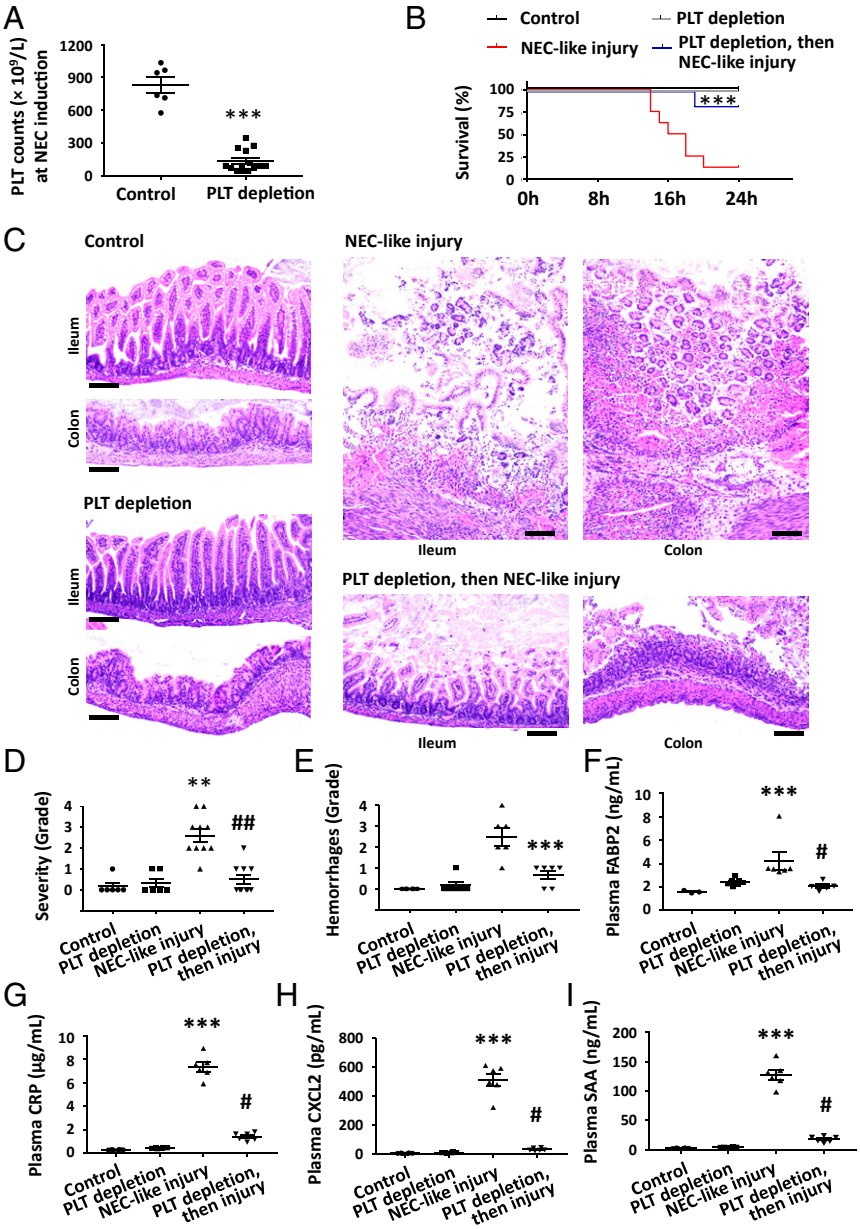

Fig. 2. Platelet depletion protects against neonatal intestinal injury. (*A*) Platelet counts in pups treated overnight with rat monoclonal anti-GP1bα (0.05 μg/g body weight, intraperitoneal) vs. isotype control. n = 7 mice treated with isotype control, 21 with anti-GP1bα. Mann–Whitney U test, ***$P < 0.001$. (*B*) Kaplan–Meier curves summarize survival data from animals in control (n = 3), intestinal injury (n = 8), platelet depletion (n = 5), and platelet depletion followed by intestinal injury (n = 6) groups. Mantel–Cox log-rank test, ***$P < 0.001$. (*C*) Representative photomicrographs (20×) show hematoxylin and eosin (H&E)-stained ileum and colon from the 4 experimental groups. (Scale bar, 100 μm.) (*D*) Severity of intestinal injury (means ± SEM) in four experimental groups and (*E*) severity of interstitial hemorrhages in the intestine (means ± SEM) graded similarly in the four groups. (*F–I*) Plasma FABP2 (*F*), CRP (*G*), CXCL2 (*H*), and SAA (*I*) in the four groups. n = 6 mice/group; Kruskal–Wallis H test with Dunn's posttest. **$P < 0.01$ and ***$P < 0.001$ vs. control; #$P < 0.05$, ##$P < 0.01$ vs. intestinal injury.

protein (PLA2AP), and the synaptosomal-associated protein 23 (SNAP23). Neonatal platelets also expressed higher levels of the ras homolog gene family-member A (RhoA), the Rho GDP-dissociation inhibitor 1 (ARHGDIA), and the Rho GDP-dissociation inhibitor 2 (ARHGDIB). A limitation of our murine model is the absence of PAR-1, which will need further investigation in human cells.

We also compared neonatal and adult plasma for endogenous thrombin antagonists. Human infants have low plasma levels of antithrombin, which may be accentuated during critical illness and may potentiate the effects of thrombin generated during tissue injury (30). To investigate the overall thrombin antagonistic activity in neonatal plasma, we spiked plasma from P10 pups and adult mice with increasing amounts of recombinant thrombin and measured thrombin activity after each addition. Addition of recombinant thrombin increased thrombin activity in neonatal plasma in a dose-dependent fashion, but produced no change in adult plasma (Fig. 4*C*; $P < 0.01$). This deficiency of thrombin antagonistic activity of neonatal mouse plasma was explained by lower plasma antithrombin and α2-macroglobulin levels in mouse pups than in adults. There was no difference in α1-antitrypsin and tissue-factor pathway inhibitor, whereas levels of heparin cofactor-II (31–33) were slightly higher in pups (Fig. 4*D*).

Intestinal Macrophages Release Tissue Factor to Activate Thrombin during Neonatal Intestinal Injury. To investigate the mechanisms of NEC-related thrombin activation, we evaluated tissue factor (TF) concentrations during NEC-like injury. Plasma TF was elevated at 2 h, preceding the observed rise at 3 h in thrombin activity (Fig. 5*A*). A transient but significant drop in intestinal TF protein levels was seen at these time points, indicating that the increased plasma TF activity was likely due to the release of preformed intestinal TF stores. Interestingly, the NEC-affected intestine showed a concomitant early rise in TF messenger RNA expression, possibly as an effort to restore the TF stores

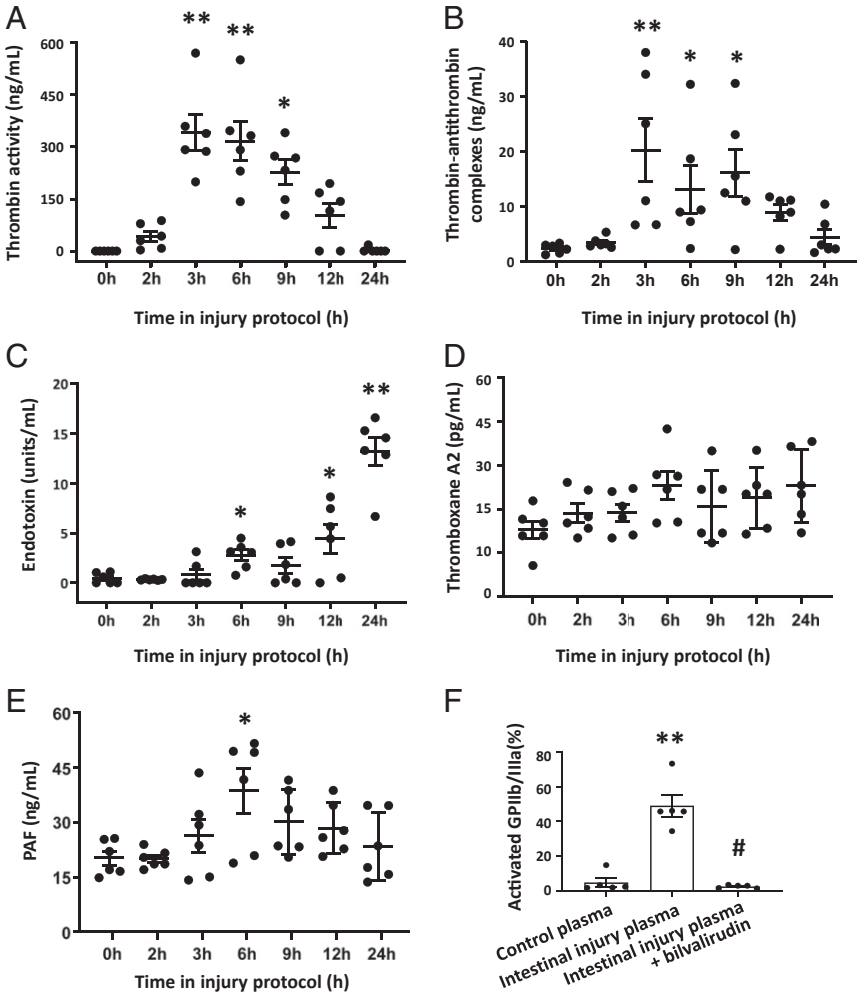

Fig. 3. Thrombin activates platelets during neonatal intestinal injury. Scatterplots (means ± SEM; top to bottom) show (*A*) plasma thrombin activity, (*B*) thrombin-antithrombin complexes, (*C*) endotoxin, (*D*) thromboxane A2, and (*E*) platelet-activating factor (PAF), measured at various time points between 0 and 24 h after initiation of intestinal injury. $n = 6$ pups. Friedman's test for repeated measures, $^{*}P < 0.05$, $^{**}P < 0.01$ vs. control. (*F*) Scatter bar diagram (means ± SEM) shows activated GPIIb/IIIa expression on platelets isolated from control pups resuspended ×45 min in plasma from control pups, pups with intestinal injury, or from pups with intestinal injury with added bivalirudin 200 ng/mL to inhibit thrombin. $n = 5$ mice/group; two runs. Kruskal–Wallis *H* test with Dunn's posttest, $^{**}P < 0.01$ vs. control; $^{\#}P < 0.05$ vs. intestinal injury.

(*SI Appendix*, Fig. S5*A*; procedure in *SI Appendix*, *Supplemental Methods*).

To ascertain the pathogenetic importance of the TF-thrombin pathway in NEC-like injury, we treated some mice with PCI-27483 (*N*-aminoiminomethyl benzimidazol aminosulfonyl dihydroxy biphenyl acetyl aspartic acid), a small-molecule inhibitor of factor VIIa in the VIIa/TF complex (34), before subjecting these animals to intestinal injury. Pretreatment with PCI-27483 blocked the early rise in plasma thrombin activity during intestinal injury (Fig. 5*B*).

We next used immunohistochemistry to identify the cellular sources of TF in the intestine. In the control group, $F4/80^{+}$ intestinal macrophages showed strong and specific TF immunoreactivity. After induction in the NEC protocol, macrophage TF expression decreased at 2 h and then recovered at 24 h (Fig. 5 *C* and *D*). We also detected delayed focal TF expression in intestinal epithelial cells (IECs) during NEC-like injury at 24 h (Fig. 5 *C* and *D* and *SI Appendix*, Fig. S5*B*). Controls for secondary antibodies are shown in *SI Appendix*, Fig. S5*C*. Interestingly, no subendothelial TF staining was seen in blood vessels (35) in the neonatal intestine. We isolated the intestinal macrophages by immunomagnetic sorting (17) and examined these cells for TF expression in vitro. In these macrophages, TF was immunolocalized to cytoplasmic granules (0.32- ± 0.01-μm diameter) and was released through constitutive and lipopolysaccharide (LPS)-induced secretion, mainly via microvesicles (Fig. 5*E*), not exosomes or the soluble fractions (*SI Appendix*, Fig. S5 *D* and *E*). Interestingly, TF expression was seen exclusively in macrophages in the neonatal, not the adult, intestine (*SI Appendix*, Fig. S5*F*).

Macrophage Toll-like Receptor 4 Is a Key Inflammatory Regulator during NEC-Like Intestinal Injury. In our NEC model, $TLR4^{-/-}$ mice were protected against NEC-related thrombocytopenia (Fig. 6*A*) and showed no mortality from intestinal inflammation (Fig. 6*B*). The absence of TLR4 reduced the severity of NEC-like injury and the severity of hemorrhages in both the ileum and colon (Fig. 6 *D* and *E*). $TLR4^{-/-}$ mice showed lower plasma levels of FABP-2 (Fig. 6*F*) and also showed lower plasma concentrations of tissue factor and levels of thrombin activity at 3 and 24 h (Fig. 6 *G* and *H*). These mice also showed less systemic inflammation with lower plasma levels of CRP, CXCL2, and SAA (*SI Appendix*, Fig. S6).

Bivalirudin-Tagged Nanoparticles Protect against Neonatal Intestinal Injury. Our studies generated important data implicating thrombin-mediated platelet activation in a pathogenetic role in NEC-like injury. Unfortunately, systemic inhibition of thrombin carries a risk of hemorrhagic complications, which is of particular concern in premature infants who are at risk for hemorrhages into the brain and other vital organs (36). Therefore, we evaluated antithrombin nanoparticles (NPs), which can bind thrombin in nascent blood clots and prevent progressive activation of the coagulation cascades and do not have increased systemic hemorrhagic complications in preclinical models (37).

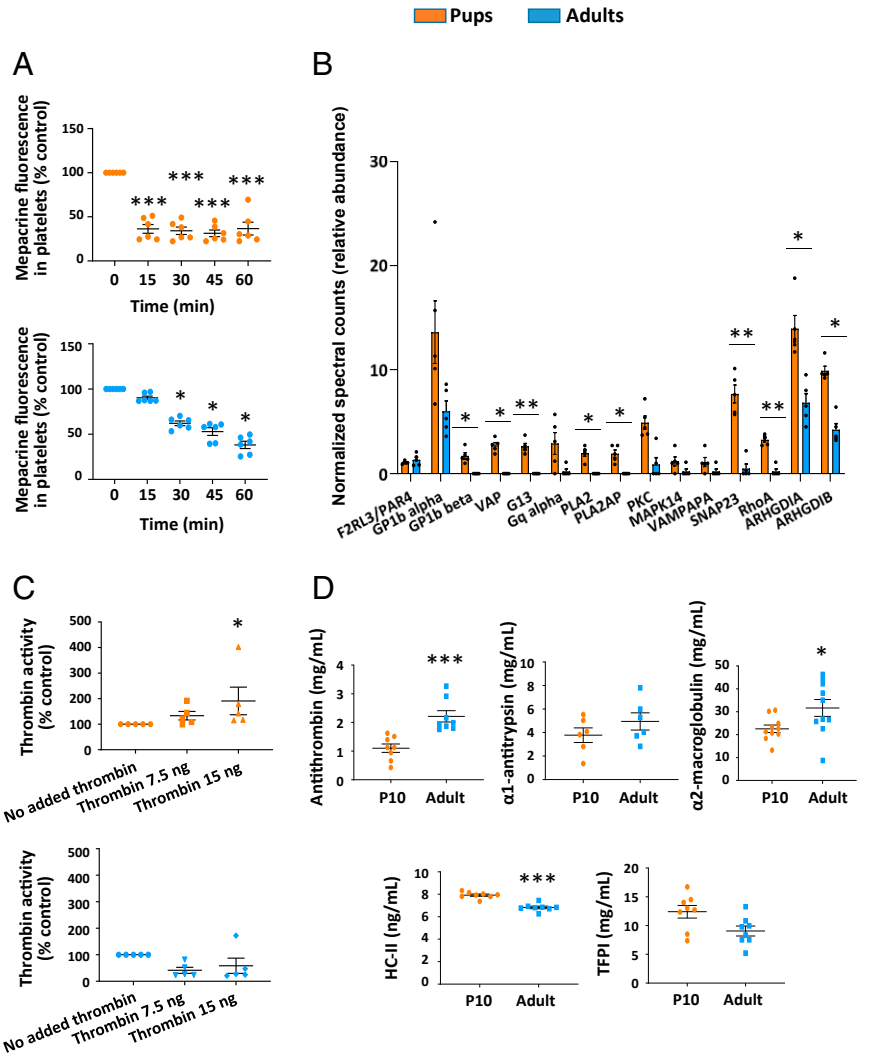

Fig. 4. Neonatal platelets are highly responsive to thrombin. (*A*) Scatterplots (means ± SEM) show mepacrine fluorescence (dense body content) of neonatal P10 (*Top*, orange circles) and adult (8 wk; *Bottom*, blue circles) platelets following thrombin stimulation. $n = 6$ mice/group; Kruskal–Wallis *U* test with Dunn's posttest; $^{*}P < 0.05$, $^{***}P < 0.001$. (*B*) Scatter bar diagrams show relative abundance of key thrombin signaling mediators in neonatal (orange bars) vs. adult (blue bars) platelets, measured by LC-MS. $n = 5$ mice/group; Kruskal–Wallis *U* test with Dunn's posttest; $^{*}P < 0.05$, $^{**}P < 0.01$. GP1b alpha, platelet glycoprotein 1b alpha chain; GP1b beta, platelet glycoprotein 1b beta chain; VASP, vasodilator stimulated phosphoprotein; G13, guanine nucleotide-binding protein, subunit alpha 13; Gq, guanine nucleotide-binding protein (g[q] subunit alpha); PLA2, cytosolic phospholipase A-2; PLA2AP, phospholipase A-2–activating protein; PKC, protein kinase C; MAPK14, mitogen-activated protein kinase p38 alpha; VAMPAPA, vesicle-associated membrane protein-associated protein A; SNAP23, synaptosomal-associated protein 23; Rho A, ras homolog gene family, member A; ARHGDIA, Rho GDP-dissociation inhibitor 1; and ARHGDIB, Rho GDP-dissociation inhibitor 2. (*C*) Scatterplots (mean ± SEM) show measured thrombin activity in plasma from P10 pups (*Top*) and adult mice (*Bottom*) spiked with recombinant mouse thrombin (0, 7.5, and 15 ng/mL). $n = 5$ mice per group; Friedman's test for repeated measures, $P < 0.01$. (*D*) Scatterplots (mean ± SEM) show plasma antithrombin, α1-antitrypsin, α2-macroglobulin, heparin cofactor-II, and tissue factor pathway inhibitor (TFPI) in plasma samples from untreated P10 and adult mice. $n = 12$ mice/group; Mann–Whitney *U* test, $^{*}P < 0.05$ and $^{***}P < 0.001$.

To confirm the activity of antithrombin NPs in vivo, we first administered control and bivalirudin-tagged perfluorocarbon-core NPs in a P10 mice ($n = 4$) at 3 h into the neonatal intestinal injury protocol (dose equivalent to 5.4×10^8 mol of bivalirudin/g body weight; predetermined optimum). As shown in Fig. 7*A*, bivalirudin NPs completely inhibited plasma thrombin activity in intestinal injury mice (treated with core NPs).

We next investigated whether bivalirudin-tagged NPs could prevent/ameliorate neonatal intestinal injury. These NPs have a half-life of ∼4 h ($n = 12$) in vivo (37), and therefore we administered two doses, the first given 1 h prior to induction of a NEC-like injury and a second dose 4 h later. Bivalirudin NPs improved survival for 24 in the initial runs (Fig. 7*B*) and up to 48 h in extended experiments ($n =$ *SI Appendix*, Fig. S7). The bivalirudin NPs also prevented thrombocytopenia (Fig. 7*C*) and reduced the severity of intestinal injury (Fig. 7 *D* and *E*) without increasing hemorrhages in the injured intestine (Fig. 7*F*). Notably, animals treated with bivalirudin NPs showed some leukocyte infiltration and submucosal edema but did not have major mucosal damage (Fig. 7*D*). Consistent with these histopathological findings, there was additional evidence for reduced epithelial injury in lower plasma FABP2 (Fig. 7*G*). The attenuation of the systemic inflammatory response was also seen with lower plasma levels of CRP, CXCL2, and SAA (Fig. 7 *H–J*).

Human NEC Shows Increased Plasma TF and TAT Complexes, and Intestinal Macrophages Express TF. To validate our findings in the mouse model, we measured circulating concentrations of tissue factor and thrombin-antithrombin complexes in patients with NEC ($n = 22$). These patients were born at gestation 29.2 ± 4.4 wk with birth weights of 1,204 ± 603 g, and blood samples were drawn on postnatal day 29.2 ± 4.2, within 48 h of disease onset. In our comparison group, we included premature infants who did not have a diagnosis of NEC ($n = 40$; gestational age of 27.3 ± 0.4 wk, birth weight 1,033 ± 52 g; blood samples collected on postnatal day 21). Patients with NEC had elevated tissue factor (Fig. 8*A*) and thrombin-antithrombin complexes (Fig. 8*B*), which increased with disease severity.

We also investigated whether macrophages in the human neonatal intestine expressed TF similarly to our observations in mouse pups (Fig. 5). We immunostained premature intestine resected for intestinal obstruction in conditions other than NEC (five samples in intestinal atresia, two samples in meconium plug, and one sample in congenital adhesions). In these conditions with uninflamed human premature intestine, macrophages showed strong cytoplasmic immunoreactivity for TF (Fig. 8 *C*, *Top*, arrows). In contrast, NEC lesion showed TF expression in macrophages, focally in epithelial cells (*Bottom*, open arrow) and in some pericryptal mesenchymal cells (*Bottom*, dashed arrows). Similar to murine pups, no perivascular TF staining was seen in the human neonatal intestine (Fig. 8*B*). The macrophage

infiltration noted in NEC lesions (*SI Appendix*, Fig. S8) has been reported previously (38). High-magnification images showed macrophage TF staining as localized in discrete cytoplasmic compartments (0.38- ± 0.01-μm diameter) similar to the murine model (Fig. 5*E*).

Tissues resected for NEC showed stronger TF immunoreactivity than did controls in epithelial cells and macrophages (Fig. 8*D*). In high-magnification images, macrophage TF expression showed a granular staining pattern, indicating possible localization to discrete cytoplasmic compartments (Fig. 8*E*). Taken together, these data validate key findings from our murine model of NEC-like injury indicating an important pathophysiological role of macrophage-derived TF and thrombin activation in human NEC.

Discussion

We present a detailed preclinical investigation of platelet activation during NEC and a therapeutic approach that merits

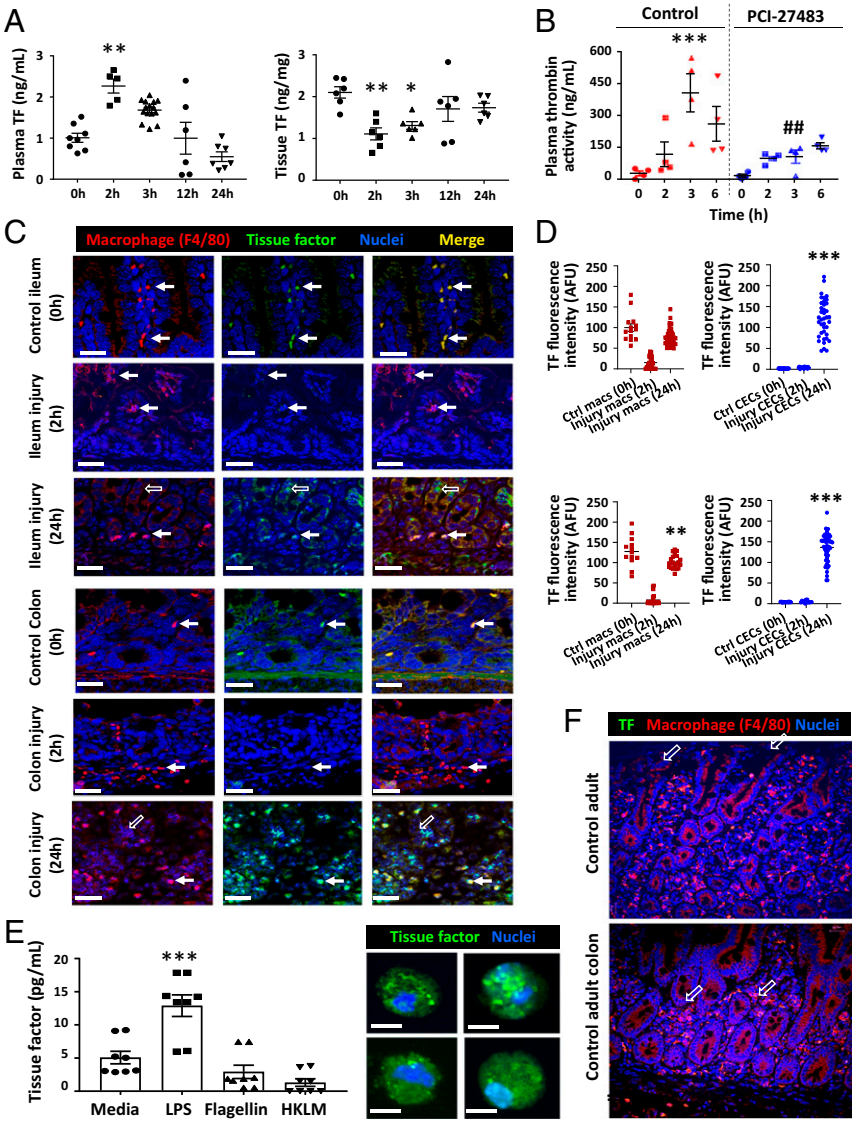

Fig. 5. Intestinal macrophages release tissue factor to activate thrombin during neonatal intestinal injury. (*A*) Scatterplots (means ± SEM) show serial tissue factor (TF) concentrations in plasma and intestinal tissue during neonatal intestinal injury. $n = 6$ mice/group; Kruskal–Wallis *H* test with Dunn's posttest, $^{*}P < 0.05$, $^{**}P < 0.01$ vs. control. (*B*) Plasma thrombin activity in pups with intestinal injury vs. pups pretreated with PCI-27483 to inhibit the tissue factor-factor VII tenase. $n = 4$ mice/group; Kruskal–Wallis *H* test with Dunn's posttest, $^{***}P < 0.001$ vs. control, $^{\#\#}P < 0.01$ vs. control treated with PCI-27483. (*C*) Representative fluorescence photomicrographs show immunoreactivity for TF (green) in F4/80^{+} (red) resident macrophages in control ileum and colon. In the injured ileum and colon, TF immunoreactivity was detectable in macrophages and epithelial cells (open arrows). (Scale bar, 25 μm.) (*D*) Scatter plots on right summarize (*Top*) TF fluorescence intensity in control IECs, control macrophages, injury IECs, and injury macrophages and (*Bottom*) in control colonic epithelial cells (CECs), control macrophages, injury CECs, and injury macrophages. $n = 5$ mice/group. Kruskal–Wallis *H* test with Dunn's posttest, $^{***}P < 0.001$ vs. control epithelial cells vs. injury epithelial cells. $^{**}P < 0.01$ vs. control macrophages vs injury macrophages. (*E*) Scatter bar diagrams (means ± SEM) summarize TF secretion by neonatal intestinal macrophages into microvesicles when cultured in media alone or after stimulation with LPS (0.5 μg/mL), *Salmonella typhimurium* flagellin (50 μg/mL), or heat-killed *Listeria monocytogenes* (10^{8}/mL) × 18 h. Kruskal–Wallis *H* test with Dunn's posttest, $^{***}P < 0.001$ vs. media alone. (*Right*) Representative fluorescence images of intestinal macrophages in the four groups show TF immunoreactivity within localized cytoplasmic compartments. (Scale bar, 5 μm.) (*F*) Representative fluorescence photomicrographs of normal adult ileum and colon show the absence of TF in F4/80^{+} (red, open arrows) macrophages in ileum (*Top*) and colon (*Bottom*). (Scale bar, 20 μm.) $n = 5$ mice.

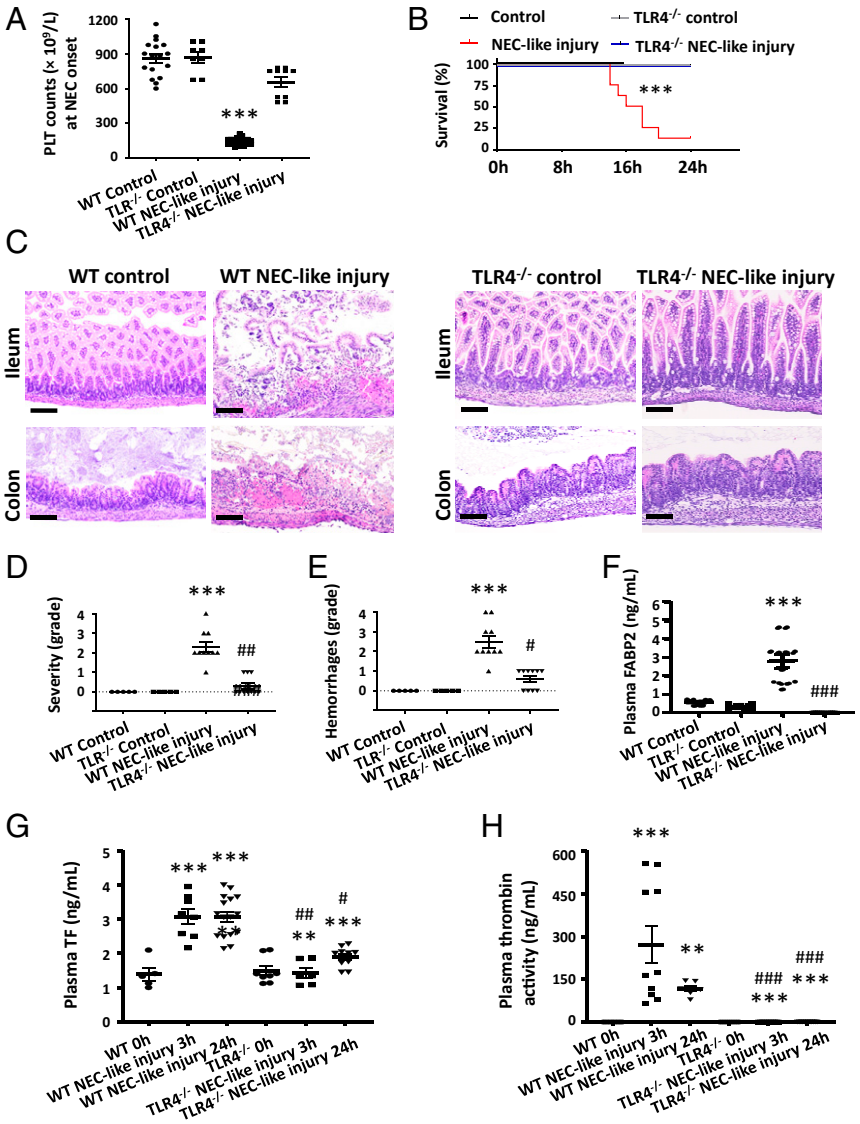

Fig. 6. Macrophage TLR4 is a key inflammatory regulator during neonatal intestinal injury. (*A*) Scatterplots show platelet counts in wild-type (WT) control ($n = 17$), TLR4$^{-/-}$ control ($n = 8$), WT mice with NEC-like injury ($n = 26$), and TLR4$^{-/-}$ mice with NEC-like injury ($n = 10$). Kruskal–Wallis *H* test with Dunn's posttest, ***$P < 0.001$. (*B*) Kaplan–Meier curves summarize survival data from animals in WT control, TLR4$^{-/-}$ control, WT mice with NEC-like injury, and TLR4$^{-/-}$ mice with NEC-like injury ($n = 8$ in each group); Mantel–Cox log-rank test. ***$P < 0.001$. (*C*) Representative photomicrographs (20×) show H&E-stained ileum and colon from the four experimental groups. (Scale bar, 100 μm.) (*D*) Severity of intestinal injury (means ± SEM) in the four experimental groups shows intestinal injury in WT and TLR4$^{-/-}$ mice. ***$P < 0.001$ vs. WT control; ##$P < 0.01$ vs. TLR4$^{-/-}$ mice with NEC-like injury. (*E*) Severity of intestinal hemorrhages (means ± SEM) in the four groups; ***$P < 0.001$; #$P < 0.05$ vs. WT mice with NEC-like injury. (*F*) FABP2 in WT control, TLR4$^{-/-}$ control, WT mice with NEC-like injury, and TLR4$^{-/-}$ mice with NEC-like injury ($n = 10$ in each group); ***$P < 0.001$ vs. WT control; ###$P < 0.001$ vs. WT mice with NEC-like injury. (*G* and *H*) Plasma levels of tissue factor and thrombin activity in WT and TLR4$^{-/-}$ mice at 0, 3, and 24 h showed lower tissue factor and thrombin activity in TLR4$^{-/-}$ mice at 3 and 24 h. $n = 10$ mice/group; Kruskal–Wallis *H* test with Dunn's posttest. **$P < 0.01$ and ***$P < 0.001$ vs. control; #$P < 0.05$, ##$P < 0.01$, ###$P < 0.001$ vs. WT mice with intestinal injury.

evaluation in human NEC. We had anticipated platelet activation to be a delayed, secondary consequence of mucosal damage and resulting bacterial translocation, but found it instead to be a thrombin-mediated, early pathogenetic event during neonatal intestinal injury. Thrombin effects may be potentiated in neonatal platelets due to unique developmental differences in downstream signaling mediators and the paucity of endogenous thrombin antagonists. We further show that resident macrophages in the neonatal intestine contain preformed TF, which was not the case in the adult intestine. Finally, we present antithrombin NPs as a specific treatment for neonatal intestinal injury. The detection of elevated plasma TF and TAT complexes in patients with NEC and of TF immunoreactivity in neonatal intestinal macrophages indicates that a similar pathway may be at work in human NEC. Prothrombotic conditions and platelet activation have been previously reported in adults with inflammatory bowel disease (39, 40). This study identifies platelet activation and thrombin as potential therapeutic targets for human NEC.

The protective effect of platelet depletion that we observed in our model of neonatal intestinal injury is intriguing. Thrombocytopenia is a frequent occurrence in confirmed NEC and is usually treated aggressively with platelet transfusions because of the risk of life-threatening hemorrhagic complications in premature infants (41–43). However, concerns remain about the possibility of harm from activated platelets, which release

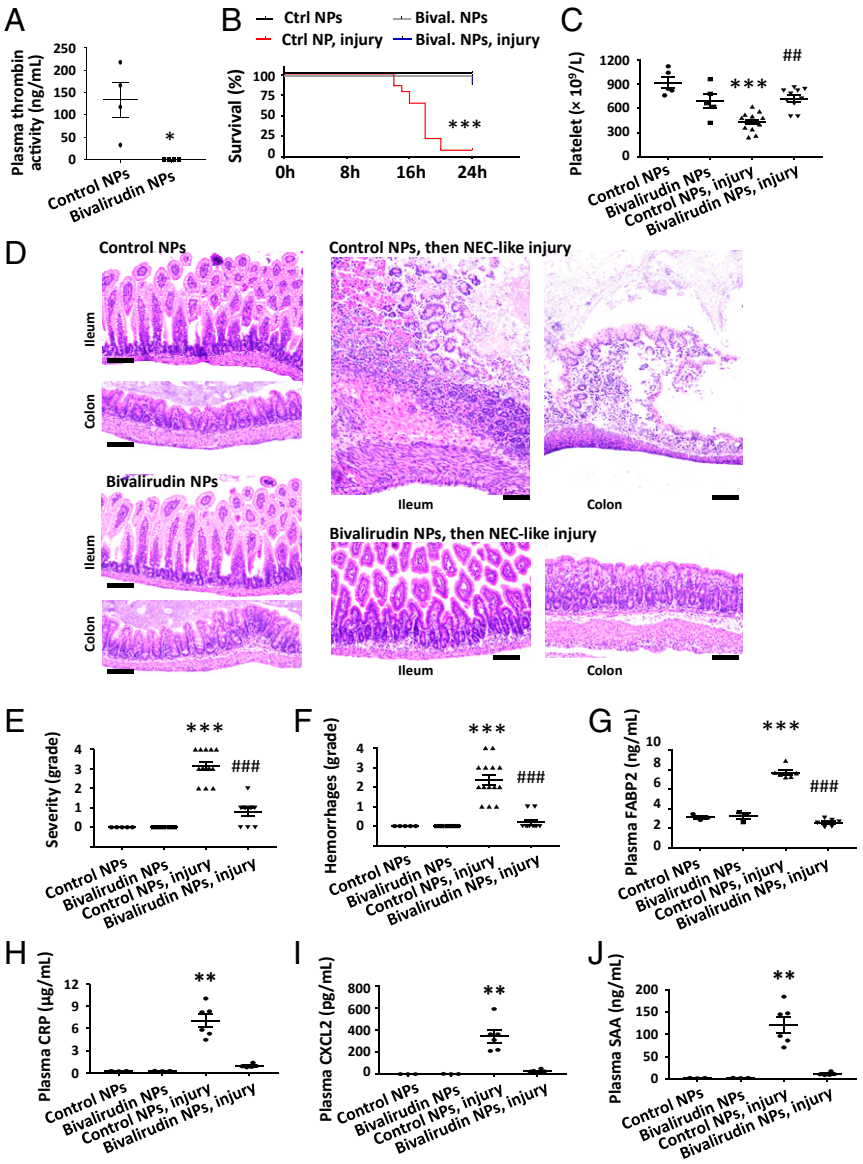

Fig. 7. Bivalirudin-tagged nanoparticles protect against neonatal intestinal injury. (*A*) Scatterplots (means ± SEM) show plasma thrombin activity in pups with intestinal injury, treated with control vs. bivalirudin-tagged nanoparticles. $n = 4$ mice/group; Mann–Whitney U test, $^{*}P < 0.05$. (*B*) Kaplan–Meier curves summarize survival in four groups: control, treated with control nanoparticles; control, treated with bivalirudin-tagged nanoparticles; control nanoparticles and intestinal injury; and bivalirudin-tagged nanoparticles and intestinal injury. $n = 6$ pups/group, Mantel–Cox log-rank test, $^{***}P < 0.001$. (*C*) Platelet counts in the four groups after killing. (*D*) Representative photomicrographs (20×) show H&E-stained ileum and colon from the above-listed experimental groups. (Scale bar, 100 μm.) (*E*) Severity of intestinal injury (means ± SEM) in the four groups. (*F*) Severity of hemorrhages in the intestine (means ± SEM) graded similarly in the four groups. (*G–J*) FABP2 (*G*), CRP (*H*), CXCL2 (*I*), and SAA (*J*) in the four groups. $n = 3$ each in control and bivalirudin nanoparticle groups, and 6 each in the control nanoparticles with injury and bivalirudin nanoparticles with injury groups; $^{**}P < 0.01$ and $^{***}P < 0.001$ vs. control; $^{\#\#\#}P < 0.001$ vs. control nanoparticle and intestinal injury group. Kruskal–Wallis H test with Dunn's posttest.

preformed vasoconstrictors and inflammatory mediators (44, 45). There is some information linking platelet transfusions with suboptimal outcomes in NEC (46–48), but most clinicians continue to use liberal transfusion thresholds because it is unclear whether the inferior outcomes in the recipients truly reflect harm from transfused platelets or merely the confounding effect of the higher severity of illness in these patients (42, 43). In a recent study, preterm infants with severe thrombocytopenia had higher mortality or major bleeding when they received platelet transfusion(s) at a platelet-count threshold of $<50 \times 10^9$/L than those transfused at platelet counts $<25 \times 10^9$/L (49). Our findings support the idea that that moderately low platelet counts may not always need prompt and aggressive correction in premature infants.

We identified thrombin as the primary mechanism for platelet activation during NEC-like intestinal injury. We had also evaluated LPS, txA2, and PAF as alternative mechanisms, but only increased thrombin activity (and increased thrombin-antithrombin complexes) antedated platelet activation. Neonatal platelets were well equipped for thrombin-activated signal transduction, and the paucity of endogenous thrombin antagonists was further likely to potentiate the biological effects of thrombin. Thrombin accumulation and thrombin-mediated platelet activation are important mechanisms for recruiting platelets into a growing hemostatic plug and could be an early event during disseminated intravascular coagulation (DIC). However, in our model, thrombin generation was independent of major tissue disruption or DIC markers such as FDPs, indicating that thrombin generation may have been a primary event unrelated to clot

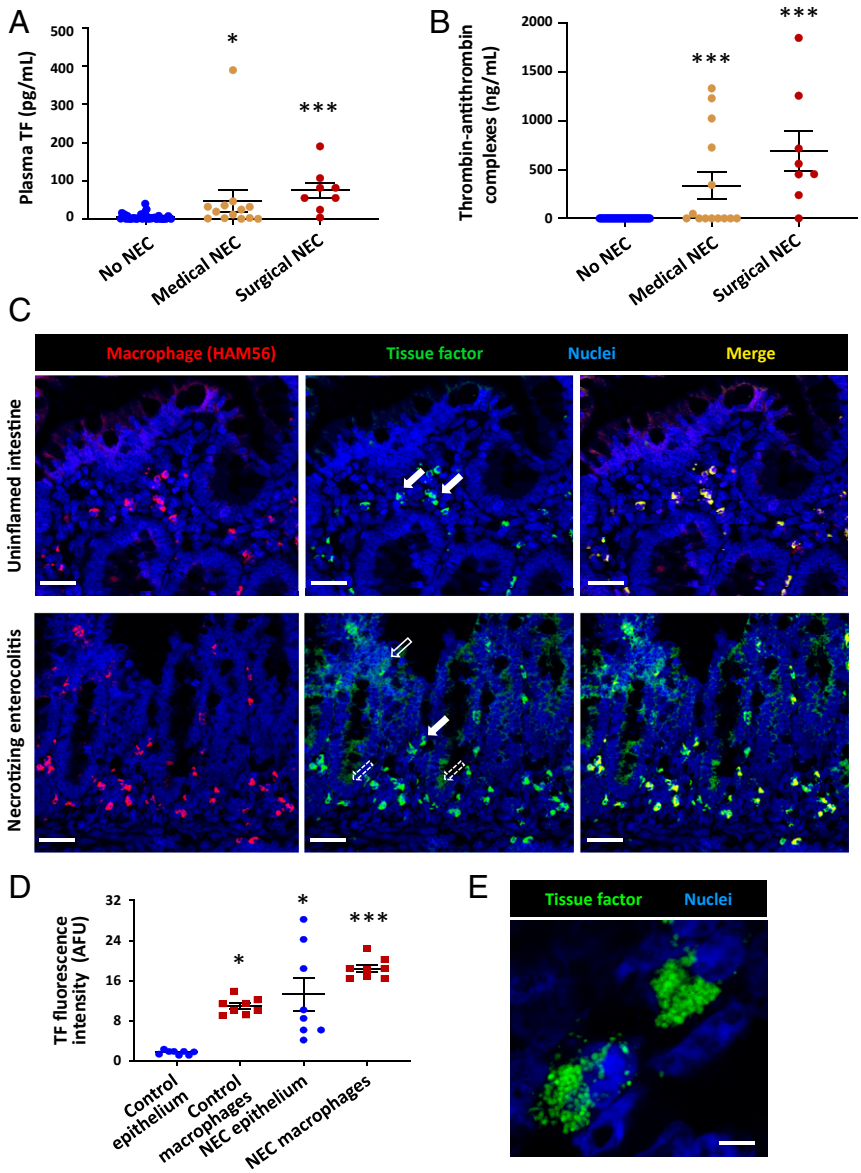

Fig. 8. Human NEC shows increased plasma TF and TAT complexes and intestinal macrophage TF. (*A*) Scatterplots (means ± SEM) summarize plasma tissue factor and (*B*) thrombin-antithrombin complexes in controls, patients with medical NEC, and those with surgical NEC. One of our patients with medical NEC had an unusually severe clinical course with culture-positive sepsis and disseminated intravascular coagulation and is seen as an outlier. NEC samples were drawn within 48 h of disease onset. $n = 22$ patients, 40 controls; Mann–Whitney *U* test, $^{***}P < 0.001$ vs. control. (*C*) Representative fluorescence photomicrographs (200×.) of uninflamed premature intestine (*Top*) show immunoreactivity for TF (green) in intestinal macrophages ($HAM56^{+}$, red). In the inflamed mucosa of NEC lesions (*Bottom*), TF immunoreactivity was more extensive and was seen in macrophages (solid arrow) and focally in epithelial cells (open arrow) and in some mesenchymal cells (dashed arrows). (Scale bar, 20 μm.) (*D*) Scatter plots below summarize epithelial and macrophage fluorescence intensity for TF in control and NEC intestine, respectively. $n = 8$ patient samples/group; Kruskal–Wallis *H* test with Dunn's posttest for group comparisons; $^{*}P < 0.05$, $^{***}P < 0.001$. (*E*) High magnification fluorescence photomicrograph (5,400×) of intestinal macrophages shows TF staining localized to discrete cytoplasmic compartments. (Scale bar, 5 μm.) $n = 8$ patients.

formation (50). This report identifies thrombin generation as a sentinel pathophysiological event in intestinal injury. Modest elevations in thrombin generation have been noted in patients with active ulcerative colitis and Crohn's disease, but thrombin is viewed as a secondary mediator of inflammation and a predictor of thrombotic events in these conditions (51, 52).

The detection of preformed TF in resident macrophages in the neonatal intestine is unusual. TF is a 30-kDa transmembrane glycoprotein that is expressed on subendothelial smooth muscle, epithelia, circulating leukocytes, and platelets (35, 53). Consistent with our own findings in adult mice, resident macrophages in the adult human gastrointestinal tract are also known to not express TF (35). In the vascular compartment, TF is believed to provide a protective hemostatic envelope; if the vessel wall is injured due to any reason, subendothelial TF is exposed and becomes available to complex with circulating factor VII, activating coagulation cascades that eventually lead to thrombin generation (53). In the neonatal intestine, we did not detect perivascular TF expression but found evidence for constitutive and inducible TF secretion by macrophages. LPS-induced macrophage TF expression is also of interest in view of increasing information linking NEC with bacterial overgrowth and

enteric dysbiosis with enrichment of Gram-negative bacteria (54). Our findings connecting TLR4-mediated signaling with TF and thrombin biogenesis further add to this equation. Another interesting aspect of macrophage TF expression was localization in well-defined cytoplasmic compartments, and at least in our ex vivo studies, these macrophages released TF specifically into microvesicles. Further study is needed to elucidate the intracellular trafficking of TF in macrophages and the role of microvesicles in transporting TF from the subepithelial lamina propria, where most macrophages are present, to the intravascular compartment.

We report successful use of antithrombin NPs to prevent/ameliorate NEC-like injury. These findings are exciting because no effective treatments are currently available for NEC and because the findings offer a viable therapeutic platform for clinical evaluation. Targeted nanomedicine allows high drug concentrations in the intended local environments while the total drug concentration and side effects are significantly reduced. As previously described (55), perfluorocarbon (PFC) NPs offer several advantages as potential therapeutic agents in critically ill infants. First, these NPs are not dependent on renal function for clearance but are cleared from the circulation by the reticuloendothelial system, and the perfluorocarbon component is ultimately vaporized through the lung (56). Second, the PFC core permits quantitative molecular imaging with fluorine magnetic resonance in vivo, which may allow assessment of regional seeding, thrombin binding, and bowel necrosis and injury.

To conclude, we report a therapeutic strategy for human NEC that merits further evaluation in human subjects. Our observations that mice with moderate thrombocytopenia had better outcomes in NEC-like injury can also be clinically relevant and call for careful evaluation of platelet transfusion thresholds in premature infants. The strengths of this study are the development of a robust preclinical model of NEC-related thrombocytopenia and the mechanistic insights that it has generated. There are some limitations: animal models may not always capture the complexity of a natural, multifactorial process such as NEC. Studies in small animals may also overlook physiological covariates such as feeding experience, comorbidities, and microbial flora, and therefore further validation in alternative disease models and clinical studies is needed.

Materials and Methods

Murine Studies. Animal studies were approved by the Institutional Animal Care and Use Committees at the University of South Florida and Johns Hopkins University. C57BL/6 mice were procured from Jackson Labs. Sample size was estimated for intestinal injury at $\alpha = 0.05$ and 80% power (Lehmann's method for non-Gaussian data). Pups were housed with and nursed by the dam throughout the study period.

NEC-like injury was induced on P10 by administering TNBS (catalog #92822, Sigma; 2 doses of 50 mg/kg in 30% ethanol, wt/vol) by gavage and rectal instillation, as described previously (1, 7, 8, 17). Controls received vehicle alone (30% ethanol) by gavage and rectal instillation. Pups from each litter were randomly assigned to these two study groups. Animals were monitored every 3 h and were euthanized if they developed physical distress or at 48 h using CO_2 inhalation followed by cervical dislocation. Histopathological grading of intestinal injury has been previously described (8) and was assigned by a blinded reviewer: grade 0 = no injury; grade 1 = mild injury; disruption of villus tips or mild separation of lamina propria in ileum; leukocyte infiltration in colon in <10% high-power fields (HPF); no structural changes. Grade 2 injury was considered moderate with midvillus disruption, clear separation of lamina propria, and/or submucosal edema and prominent with leukocyte infiltration in the colon in ≤50% HPF, crypt elongation, mucosal thickening, superficial ulcerations. Grade 3 injury was considered severe with transmural injury in ileum and marked in leukocyte infiltration in >50% HPF, elongated and distorted crypts, bowel-wall thickening, and extensive ulcerations.

The severity of gut mucosal hemorrhages was graded on a four-point scale: grade 0 = no hemorrhage; grade 1 = hemorrhage in villus tips or upper lamina propria in the ileum or subepithelial colon in <10% HPF; grade 2 hemorrhage was moderate, affecting most of the villi, 10 to 30% of the subepithelial colon, or extending into the lamina propria. Grade 3 hemorrhage was considered severe with submucosal involvement of the ileum or with >50% of the colon. Grade 4 hemorrhage was transmural and involved both the ileum and colon.

In some studies, we administered rat anti-mouse GP1bα (0.05 μg/g body weight, intraperitoneal; Emfret Analytics; catalog #R300) 12 h before administration of TNBS to deplete circulating platelets. Adult C57BL/6 mice ($n = 10$; weight: mean ± SEM 25.2 ± 1.8 g) used for comparison also received two doses of 50 mg/kg TNBS similar to pups; blood samples were drawn at 0 to 6 h.

To evaluate the TF-thrombin pathway in NEC-like injury, we treated some mice with PCI-27483 (*N*-aminoiminomethyl benzimidazol aminosulfonyl dihydroxy biphenyl acetyl aspartic acid) (34) before subjecting these animals to intestinal injury. PCI-27483 (0.5 mg/mL) was dissolved 1:1 in dimethylsulfoxide:phosphate-buffered saline (pH 7.2).

Platelet Isolation and Measurements. Blood was drawn from anterior facial vein puncture (57), and platelets were enumerated using a Sysmex XT-2000iV hematology analyzer (details in *SI Appendix*). Expression of activated integrin GPIIb/IIIa, CD62P, CD41/GPIIb, CD61/integrin αvβ3, and CD31/PECAM-1 were measured by flow cytometry using the following fluorescence-labeled antibodies: clone JON/A against activated integrin GPIIb/IIIa (Emfret, catalog #M023-2) and anti-CD62P, anti-CD41/GPIIb, CD61/integrin αvβ3, and CD31/PECAM-1 (BioLegend; catalog #148301, 133907, 104311, 102413, respectively). Platelet aggregation was measured by the impedance method and ATP release by luminometry using a two-channel Chrono-Log lumi-aggregometer (model 700, Chrono-Log). Mepacrine staining and fluorescence measurements (436/525 nm), and transmission electron microscopy (TEM) methods are described in *SI Appendix*. Neonatal (P10) and adult (3 mo) murine platelets ($n = 5$ mice/group) were evaluated for thrombin-signaling pathway proteins by LC-MS analysis (58).

Human Plasma and Tissue Samples. De-identified, archived plasma and serum samples from premature infants with a diagnosis of NEC (Bell stages 2 and 3) and controls were obtained from existing biorepositories at Johns Hopkins University and at the University of Texas Medical Branch at Galveston. We also used de-identified archived paraffin-embedded tissue specimens of human NEC and uninflamed human premature intestine resected for indications other than NEC, for immunohistochemistry. All studies were approved by the respective Institutional Review Boards.

Chemicals. PPACK dihydrochloride and bivalirudin trifluoroacetate assays were purchased from Sigma (catalog #520222 and #SML1051, respectively).

Quantitative Protein Measurements. Commercially available enzyme immunoassays were used to measure murine FABP2, CXCL2, CRP, SAA, txA2, PAF, α2-macroglobulin, heparin cofactor-II, F3/tissue factor, tissue factor pathway inhibitor, TAT complexes, and fibrin degradation products (MyBioSource; catalog #MBS010793, MBS717328, MBS062877, MBS776916, MBS777014, MBS776759, MBS2020230, MBS265219, MBS162963, MBS162794, MBS777009, MBS161152); antithrombin and α1-antitrypsin (Innovative Research; catalog # IRAPKT017, IRKTAH1147). Thrombin activity was measured by a fluorometric assay (Abcam; catalog #ab197006). Plasma endotoxin levels were quantified by the Limulus Amebocyte Lysate assay (ThermoFisher Scientific; catalog #88282). Human TAT complexes and tissue factor were measured by enzyme immunoassay (Abcam; catalog #ab108907; ab108903).

Thromboxane A2 enzyme immunoassay kits were purchased from Aviva Systems Biology (catalog #OKEH02590) and PAF enzyme immunoassay from Biovision (catalog #E4631).

Immunofluorescence Imaging. Immunofluorescence imaging was performed as described previously (17, 59) and in *SI Appendix*. The following primary antibodies were used: rat anti-mouse F4/80 (clone BM8, ThermoFisher), rabbit anti-mouse/human tissue factor (Abcam; catalog #ab104513), or mouse anti-human macrophage marker HAM56 (ThermoFisher; catalog #14–6548-93).

Murine Intestinal Macrophages. Murine intestinal macrophages were isolated from intestinal tissue by immunomagnetic separation as described in *SI Appendix*.

Culture supernatants were fractionated to first separate microvesicles by centrifugation at 20,000 × *g* for 40 min at room temperature (Sorvall WX ultracentrifuge, ThermoFisher) and then to separate exosomes by another centrifugation at 100,000 × *g* for 1 h at 4 °C (60).

Perfluorocarbon NPs. Perfluorocarbon NPs were formulated and conjugated with bivalirudin as described previously (55). The average NP diameter was 269.8 nm, polydispersity 0.146, and zeta potential −20 mV.

Data Availability. All data and associated protocols are included in this article and *SI Appendix*.

ACKNOWLEDGMENTS. The study was made possible by NIH awards HL133022 and HL124078 (to A.M.) and DK102691 and HL073646 (to S.A.W.). We thank Sysmex America, Inc. for the instrument loan (Sysmex XT-2000iV) and Dr. Jack Widness for the introduction to the Sysmex team and to veterinary hematology analyzers.

1. K. Namachivayam, K. MohanKumar, L. Garg, B. A. Torres, A. Maheshwari, Neonatal mice with necrotizing enterocolitis-like injury develop thrombocytopenia despite increased megakaryopoiesis. *Pediatr. Res.* **81**, 817–824 (2017).
2. J. Neu, W. A. Walker, Necrotizing enterocolitis. *N. Engl. J. Med.* **364**, 255–264 (2011).
3. R. M. Patel *et al.*; Eunice Kennedy Shriver National Institute of Child Health and Human Development Neonatal Research Network, Causes and timing of death in extremely premature infants from 2000 through 2011. *N. Engl. J. Med.* **372**, 331–340 (2015).
4. T. T. B. Ho *et al.*, Dichotomous development of the gut microbiome in preterm infants. *Microbiome* **6**, 157 (2018).
5. T. T. B. Ho *et al.*, Enteric dysbiosis and fecal calprotectin expression in premature infants. *Pediatr. Res.* **85**, 361–368 (2019).
6. J. B. Fundora, P. Guha, D. R. Shores, M. Pammi, A. Maheshwari, Intestinal dysbiosis and necrotizing enterocolitis: Assessment for causality using Bradford Hill criteria. *Pediatr. Res.* **87**, 235–248 (2020).
7. K. MohanKumar *et al.*, Trinitrobenzene sulfonic acid-induced intestinal injury in neonatal mice activates transcriptional networks similar to those seen in human necrotizing enterocolitis. *Pediatr. Res.* **81**, 99–112 (2017).
8. K. MohanKumar *et al.*, Gut mucosal injury in neonates is marked by macrophage infiltration in contrast to pleomorphic infiltrates in adult: Evidence from an animal model. *Am. J. Physiol. Gastrointest. Liver Physiol.* **303**, G93–G102 (2012).
9. C. Zhang *et al.*, Paneth cell ablation in the presence of Klebsiella pneumoniae induces necrotizing enterocolitis (NEC)-like injury in the small intestine of immature mice. *Dis. Model. Mech.* **5**, 522–532 (2012).
10. K. MohanKumar *et al.*, A murine neonatal model of necrotizing enterocolitis caused by anemia and red blood cell transfusions. *Nat. Commun.* **10**, 3494 (2019).
11. J. J. Hutter, Jr, W. E. Hathaway, E. R. Wayne, Hematologic abnormalities in severe neonatal necrotizing enterocolitis. *J. Pediatr.* **88**, 1026–1031 (1976).
12. A. Maheshwari, Immunologic and hematological abnormalities in necrotizing enterocolitis. *Clin. Perinatol.* **42**, 567–585 (2015).
13. C. C. Patel, Hematologic abnormalities in acute necrotizing enterocolitis. *Pediatr. Clin. North Am.* **24**, 579–584 (1977).
14. M. Ververidis *et al.*, The clinical significance of thrombocytopenia in neonates with necrotizing enterocolitis. *J. Pediatr. Surg.* **36**, 799–803 (2001).
15. R. S. Nickel, C. D. Josephson, Neonatal transfusion medicine: Five major unanswered research questions for the twenty-first century. *Clin. Perinatol.* **42**, 499–513 (2015).
16. P. Alex *et al.*, Distinct cytokine patterns identified from multiplex profiles of murine DSS and TNBS-induced colitis. *Inflamm. Bowel Dis.* **15**, 341–352 (2009).
17. K. MohanKumar *et al.*, Smad7 interrupts TGF-β signaling in intestinal macrophages and promotes inflammatory activation of these cells during necrotizing enterocolitis. *Pediatr. Res.* **79**, 951–961 (2016).
18. R. D. Christensen *et al.*, Thrombocytopenia among extremely low birth weight neonates: Data from a multihospital healthcare system. *J. Perinatol.* **26**, 348–353 (2006).
19. V. L. Baer, D. K. Lambert, E. Henry, R. D. Christensen, Severe thrombocytopenia in the NICU. *Pediatrics* **124**, e1095–e1100 (2009).
20. W. Bergmeier *et al.*, Flow cytometric detection of activated mouse integrin alphaIIbbeta3 with a novel monoclonal antibody. *Cytometry* **48**, 80–86 (2002).
21. J. Simák, K. Holada, J. Janota, Z. Stranák, Surface expression of major membrane glycoproteins on resting and TRAP-activated neonatal platelets. *Pediatr. Res.* **46**, 445–449 (1999).
22. J. E. Wall *et al.*, A flow cytometric assay using mepacrine for study of uptake and release of platelet dense granule contents. *Br. J. Haematol.* **89**, 380–385 (1995).
23. K. MohanKumar *et al.*, Intestinal epithelial apoptosis initiates gut mucosal injury during extracorporeal membrane oxygenation in the newborn piglet. *Lab. Invest.* **94**, 150–160 (2014).
24. P. C. Ng, Biomarkers of necrotising enterocolitis. *Semin. Fetal Neonatal Med.* **19**, 33–38 (2014).
25. T. D. Gladwell, Bivalirudin: A direct thrombin inhibitor. *Clin. Ther.* **24**, 38–58 (2002).
26. A. H. Schmaier, F. J. Meloni, W. Nawarawong, Y. P. Jiang, PPACK-thrombin is a noncompetitive inhibitor of alpha-thrombin binding to human platelets. *Thromb. Res.* **67**, 479–489 (1992).
27. M. M. Mull, W. E. Hathaway, Altered platelet function in newborns. *Pediatr. Res.* **4**, 229–237 (1970).
28. B. Shenkman *et al.*, Increased neonatal platelet deposition on subendothelium under flow conditions: The role of plasma von Willebrand factor. *Pediatr. Res.* **45**, 270–275 (1999).
29. E. Stokhuijzen *et al.*, Differences between platelets derived from neonatal cord blood and adult peripheral blood assessed by mass spectrometry. *J. Proteome Res.* **16**, 3567–3575 (2017).
30. M. J. Manco-Johnson, Neonatal antithrombin III deficiency. *Am. J. Med.* **87** (3B), 49S–52S (1989).
31. D. O'Keeffe *et al.*, The heparin binding properties of heparin cofactor II suggest an antithrombin-like activation mechanism. *J. Biol. Chem.* **279**, 50267–50273 (2004).
32. D. M. Tollefsen, Heparin cofactor II deficiency. *Arch. Pathol. Lab. Med.* **126**, 1394–1400 (2002).
33. P. Golino, The inhibitors of the tissue factor:factor VII pathway. *Thromb. Res.* **106**, V257–V265 (2002).
34. A. Gómez-Outes *et al.*, New parenteral anticoagulants in development. *Ther. Adv. Cardiovasc. Dis.* **5**, 33–59 (2011).
35. T. A. Drake, J. H. Morrissey, T. S. Edgington, Selective cellular expression of tissue factor in human tissues. Implications for disorders of hemostasis and thrombosis. *Am. J. Pathol.* **134**, 1087–1097 (1989).
36. M. L. Buck, Bivalirudin as an alternative to heparin for anticoagulation in infants and children. *J. Pediatr. Pharmacol. Ther.* **20**, 408–417 (2015).
37. J. Myerson, L. He, G. Lanza, D. Tollefsen, S. Wickline, Thrombin-inhibiting perfluorocarbon nanoparticles provide a novel strategy for the treatment and magnetic resonance imaging of acute thrombosis. *J. Thromb. Haemost.* **9**, 1292–1300 (2011).
38. J. I. Remon *et al.*, Depth of bacterial invasion in resected intestinal tissue predicts mortality in surgical necrotizing enterocolitis. *J. Perinatol.* **35**, 755–762 (2015).
39. S. Danese *et al.*, Inflammation and coagulation in inflammatory bowel disease: The clot thickens. *Am. J. Gastroenterol.* **102**, 174–186 (2007).
40. A. Denadai-Souza *et al.*, Functional proteomic profiling of secreted serine proteases in health and inflammatory bowel disease. *Sci. Rep.* **8**, 7834 (2018).
41. S. J. Stanworth *et al.*; Platelets and Neonatal Transfusion Study Group, Prospective, observational study of outcomes in neonates with severe thrombocytopenia. *Pediatrics* **124**, e826–e834 (2009).
42. C. D. Josephson *et al.*, Platelet transfusion practices among neonatologists in the United States and Canada: Results of a survey. *Pediatrics* **123**, 278–285 (2009).
43. M. Cremer *et al.*, Platelet transfusions in neonates: Practices in the United States vary significantly from those in Austria, Germany, and Switzerland. *Transfusion* **51**, 2634–2641 (2011).
44. C. E. Collins, M. R. Cahill, A. C. Newland, D. S. Rampton, Platelets circulate in an activated state in inflammatory bowel disease. *Gastroenterology* **106**, 840–845 (1994).
45. M. R. Thomas, R. F. Storey, The role of platelets in inflammation. *Thromb. Haemost.* **114**, 449–458 (2015).
46. A. B. Kenton *et al.*, Platelet transfusions in infants with necrotizing enterocolitis do not lower mortality but may increase morbidity. *J. Perinatol.* **25**, 173–177 (2005).
47. M. G. Garcia *et al.*, Epidemiologic and outcome studies of patients who received platelet transfusions in the neonatal intensive care unit. *J. Perinatol.* **21**, 415–420 (2001).
48. V. L. Baer *et al.*, Do platelet transfusions in the NICU adversely affect survival? Analysis of 1600 thrombocytopenic neonates in a multihospital healthcare system. *J. Perinatol.* **27**, 790–796 (2007).
49. A. Curley *et al.*, Randomized trial of platelet-transfusion thresholds in neonates. *N. Engl. J. Med.* **380**, 242–251 (2019).
50. K. E. Brummel, S. G. Paradis, S. Butenas, K. G. Mann, Thrombin functions during tissue factor-induced blood coagulation. *Blood* **100**, 148–152 (2002).
51. S. Saibeni *et al.*, Increased thrombin generation in inflammatory bowel diseases. *Thromb. Res.* **125**, 278–282 (2010).
52. A. Deutschmann *et al.*, Increased procoagulant function of microparticles in pediatric inflammatory bowel disease: Role in increased thrombin generation. *J. Pediatr. Gastroenterol. Nutr.* **56**, 401–407 (2013).
53. H. Zelaya, A. S. Rothmeier, W. Ruf, Tissue factor at the crossroad of coagulation and cell signaling. *J. Thromb. Haemost.* **16**, 1941–1952 (2018).
54. M. Pammi *et al.*, Intestinal dysbiosis in preterm infants preceding necrotizing enterocolitis: A systematic review and meta-analysis. *Microbiome* **5**, 31 (2017).
55. J. Chen *et al.*, Antithrombin nanoparticles improve kidney reperfusion and protect kidney function after ischemia-reperfusion injury. *Am. J. Physiol. Renal Physiol.* **308**, F765–F773 (2015).
56. J. Chen, G. M. Lanza, S. A. Wickline, Quantitative magnetic resonance fluorine imaging: Today and tomorrow. *Wiley Interdiscip. Rev. Nanomed. Nanobiotechnol.* **2**, 431–440 (2010).
57. A. L. Sørensen *et al.*, Role of sialic acid for platelet life span: Exposure of beta-galactose results in the rapid clearance of platelets from the circulation by asialoglycoprotein receptor-expressing liver macrophages and hepatocytes. *Blood* **114**, 1645–1654 (2009).
58. A. J. Worth *et al.*, LC-MS analysis of human platelets as a platform for studying mitochondrial metabolism. *J. Vis. Exp.*, e53941 (2016).
59. K. Namachivayam *et al.*, Smad7 inhibits autocrine expression of TGF-β2 in intestinal epithelial cells in baboon necrotizing enterocolitis. *Am. J. Physiol. Gastrointest. Liver Physiol.* **304**, G167–G180 (2013).
60. M. T. Aatonen *et al.*, Isolation and characterization of platelet-derived extracellular vesicles. *J. Extracell. Vesicles* **3**, 3 (2014).